Coulomb stress changes in the South Iceland Seismic Zone due to two large earthquakes in June 2000

Thóra Árnadóttir,[1] Sigurjón Jónsson,[2] Rikke Pedersen,[1] and Gunnar B. Gudmundsson[3]

Received 22 October 2002; revised 23 December 2002; accepted 3 February 2003; published 5 March 2003.

[1] The South Iceland Seismic Zone experienced the largest earthquakes for 88 years in June 2000, with a M_S = 6.6 event on June 17, followed by another M_S = 6.6 earthquake on June 21. These events occurred on two parallel N-S striking, right-lateral strike slip faults, separated by about 17 km. We calculate the static Coulomb stress change for the June 17 and 21 earthquakes using a distributed slip model derived from joint inversion of InSAR and GPS data. We find that the static stress change caused by the June 17 event is about 0.1 MPa at the location of the June 21 hypocenter, promoting failure on the second fault. Locations of aftershocks agree well with areas of increased Coulomb failure stress. Our calculations indicate that positive stress changes due to the two earthquakes make the area west of the June 21 rupture the most likely site of the next large earthquake in South Iceland. *INDEX TERMS:* 1242 Geodesy and Gravity: Seismic deformations (7205); 7209 Seismology: Earthquake dynamics and mechanics; 7215 Seismology: Earthquake parameters; 7230 Seismology: Seismicity and seismotectonics; 7260 Seismology: Theory and modeling. **Citation:** Árnadóttir, T., S. Jónsson, R. Pedersen, and G. B. Gudmundsson, Coulomb stress changes in the South Iceland Seismic Zone due to two large earthquakes in June 2000, *Geophys. Res. Lett.*, *30*(5), 1205, doi:10.1029/2002GL016495, 2003.

1. Introduction

[2] Iceland is located on the mid-Atlantic ridge, which continues on land as the Reykjanes Peninsula (RP) oblique rift zone. The plate spreading across south Iceland occurs in two parallel rift zones, the Western Volcanic Zone (WVZ) and the Eastern Volcanic Zone (EVZ). The two volcanic zones are connected by a left-lateral E-W transform zone, the South Iceland Seismic Zone (SISZ) (Figure 1). The relative plate motion across the SISZ is accommodated by right-lateral strike slip motion on many parallel N-S oriented faults, rather than one E-W transform fault [*Einarsson and Eirksson*, 1982; *Einarsson et al.*, 1981].

[3] Many large ($M_S \geq 6$) earthquakes have occurred in the SISZ since Iceland was settled in the ninth century A.D. Historical accounts describe sequences of large earthquakes over a period of days to years, starting with an earthquake in the eastern part of the SISZ and continuing with events of equal or smaller magnitude further west. The time interval between large earthquake sequences in the SISZ ranges between 45 and 112 years [*Einarsson et al.*, 1981]. Such series of earthquakes occurred for example in 1630–1633, 1732–1734, 1784, 1896 and 2000. The largest historical earthquake, with estimated M_S = 7.1, occurred on August 14, 1784, and was followed two days later by a second event of M_S = 6.7, approximately 30 km to the west. From August 26 to September 6, 1896, five M_S = 6.0–6.9 earthquakes swept through the SISZ, causing widespread damage. Several large historical earthquakes in the SISZ have, however, occurred as single events. The events in 1726, 1829, and 1912 are examples of single earthquakes that occurred in the eastern part of the SISZ. The 1912 event (M_S = 7.0) was the first SISZ earthquake to be instrumentally recorded [*Bjarnason et al.*, 1993]. Following the 1912 earthquake, the SISZ was seismically relatively quiet until June 2000.

[4] The June 2000 sequence started with an earthquake of M_S = 6.6 at 15:40:41 UTC on June 17, 2000 (NEIC). The hypocenter was located at 63.975°N, 20.370°W and 6.3 km depth. Seismicity increased over a large area in SW Iceland following the June17 mainshock. The June 17 mainshock probably triggered significant slip on three faults on the Reykjanes Peninsula [*Pagli et al.*, 2003]. A second large event with M_S = 6.6 occurred on June 21, 2000 (00:51:47 UTC), located about 17 km west of the June 17 rupture, at 63.977°N, 20.713°W and 5.1 km depth (Figure 1).

[5] Signals from the earthquakes were observed with several local networks: the SIL digital seismic network, a strong motion network, a volumetric strain meter network, and the continuous GPS network in Iceland. The earthquakes caused significant pressure changes in geothermal reservoirs in an extensive area, with local changes that are consistent with the focal mechanisms of the two largest events [*Björnsson et al.*, 2001]. Surface ruptures were observed for the events in the SISZ, and on Reykjanes Peninsula, indicating rupture on N-S trending faults (A. Clifton, personal communication, 2002). Crustal deformation caused by the June 17 and 21earthquakes was measured with network GPS [*Árnadóttir et al.*, 2001] and Interferometric Synthetic Aperture Radar (InSAR) [*Pedersen et al.*, 2001], and the data used to estimate best fit fault geometries assuming uniform or simple slip models. In a more recent study the InSAR and GPS data were combined to estimate the best fit fault geometries and distributed slip models for the two earthquakes [*Pedersen et al.*, 2003].

[6] In this study we use the distributed slip models from *Pedersen et al.* [2003] to calculate the static stress change due to the June 17 mainshock to determine whether it was likely to have promoted failure on the June 21 fault. We also

[1]Nordic Volcanological Institute, Reykjavík, Iceland.
[2]Harvard University, Department of Earth and Planetary Sciences, Cambridge, Massachusetts, USA.
[3]Icelandic Meteorological Office, Reykjavík, Iceland.

Copyright 2003 by the American Geophysical Union.
0094-8276/03/2002GL016495$05.00

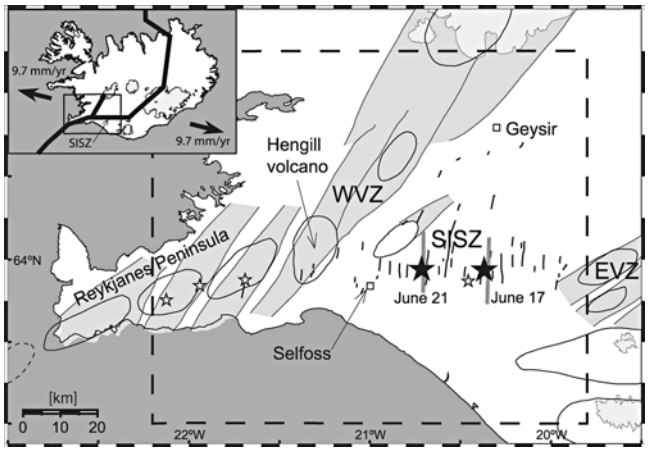

Figure 1. Map of the main tectonic features of southwest Iceland. The epicenters of the June 17 and June 21, 2000, earthquakes are shown with large black stars and the four largest aftershocks on June 17 are noted with small gray stars. The locations of the June 17 and 21 fault models are marked by bold gray lines, while mapped N-S faults caused by historical events are shown with black lines [*Einarsson and Sæmundsson*, 1987]. The locations of the South Iceland Seismic Zone (SISZ), Western Volcanic Zone (WVZ), and the Eastern Volcanic Zone (EVZ) are also shown. Light shaded areas are individual spreading segments with associated central volcanoes. Dashed box marks the area covered in Figures 3 and 4. The inset shows the plate-boundary across Iceland and the NUVEL-1A plate motion. The location of Figure 1 is indicated by a box.

examine the correlation between the aftershock locations and the stress changes caused by the two main earthquakes.

2. Coulomb Failure Stress

[7] Many studies have shown that static stress changes as small as 0.01 MPa (0.1 bar) caused by large earthquakes affect aftershock locations and may trigger subsequent events in a crust near to the critical state of failure [e.g., *Harris*, 1998, and references therein]. This has been demonstrated using the Coulomb failure criterion, where failure will occur on a plane when the applied stress increment, defined as the change in Coulomb failure stress (ΔCFS) [e.g., *Harris*, 1998]

$$\Delta CFS = \Delta\tau_s + \mu(\Delta\sigma_n + \Delta p), \tag{1}$$

exceeds a threshold value, where $\Delta\tau_s$ is the change in shear stress resolved in the slip direction of a fault that may fail in a subsequent earthquake, $\Delta\sigma_n$ is the change in normal stress due to the first earthquake, perpendicular to the subsequent earthquake fault plane (positive for extension), Δp is the change in pore pressure, and μ is the coefficient of friction, which ranges from 0.6 to 0.8 for most rocks [e.g., *Harris*, 1998, and references therein]. The change in pore pressure due to a change in stress under undrained conditions (i.e., where there is no fluid flow) in a homogeneous isotropic poroelastic medium is given by [*Rice and Cleary*, 1976]

$$\Delta p = -\frac{B}{3}\Delta\sigma_{kk}, \tag{2}$$

where $\sigma_{kk} = \sigma_{xx} + \sigma_{yy} + \sigma_{zz}$ is the volumetric stress, and B is the Skempton coefficient of the rock-fluid mixture. Theoretically, B ranges from 0 to 1.0 depending on the level of fluid saturation, but experimental values range from 0.47 to 1.0 [e.g., *Harris*, 1998, and references therein]. Substituting Equation 2 into 1 gives the Coulomb failure stress change for an isotropic fault zone model [*Beeler et al.*, 2000; *Cocco and Rice*, 2002]:

$$\Delta CFS = \Delta\tau_s + \mu\left(\Delta\sigma_n - \frac{B}{3}\Delta\sigma_{kk}\right). \tag{3}$$

A positive ΔCFS implies an increase in Coulomb failure stress, indicating that the first earthquake brought the second fault closer to failure.

[8] We calculate the change in Coulomb failure stress from Equation 3, for the June 17 and 21, 2000 earthquakes, using a distributed slip fault model (Figure 2) obtained by joint inversion of InSAR and GPS data [*Pedersen et al.*, 2003]. We calculate the ΔCFS in an elastic half-space for vertical, N-S, right-lateral strike slip faults, representing the fault geometry and slip direction estimated for the June 21 earthquake. We use a Poisson's ratio of $\nu = 0.28$, a shear modulus of 30 GPa, a coefficient of friction $\mu = 0.75$ and a Skempton coefficient B = 0.5.

[9] The June 17 mainshock increased the Coulomb failure stress by about 0.1 MPa at the hypocenter location of the June 21 shock, increasing the probabililty of the occurrence of the second event [*Toda et al.*, 1998] (Figure 3). Aftershock locations from June 17 to June 21, correlate well with areas of increased *CFS* (Figure 3). Four M $\sim$ 5 aftershocks occurred within 5 minutes of the June 17 mainshock (white stars in Figure 3). The largest aftershock in the SISZ (located about 5 km SW of the mainshock epicenter) occurred at 15:42:50 UTC, in an area where the *CFS* increased by about 0.6 MPa. Three events were triggered on Reykjanes Peninsula, progressively further west of the June 17 mainshock (Figure 3). The first two events occurred 26 and 30 seconds after the mainshock, but the third event occurred about 5 minutes later. The timing of the events suggest that the first two were triggered by the surface waves from the mainshock, as was widely observed following the 1992 Landers earthquake [e.g., *Spudich et al.*, 1995].

[10] A number of aftershocks occurred in the Hengill volcanic area following the June 17 mainshock (Figure 3).

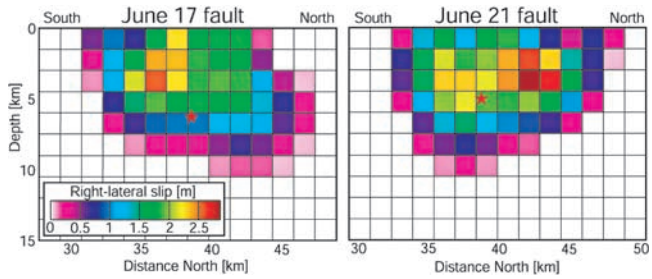

Figure 2. Right-lateral fault slip models for the June 17 and June 21 mainshocks derived from joint inversion of InSAR and GPS data [*Pedersen et al.*, 2003]. The stars show the mainshock hypocenter locations.

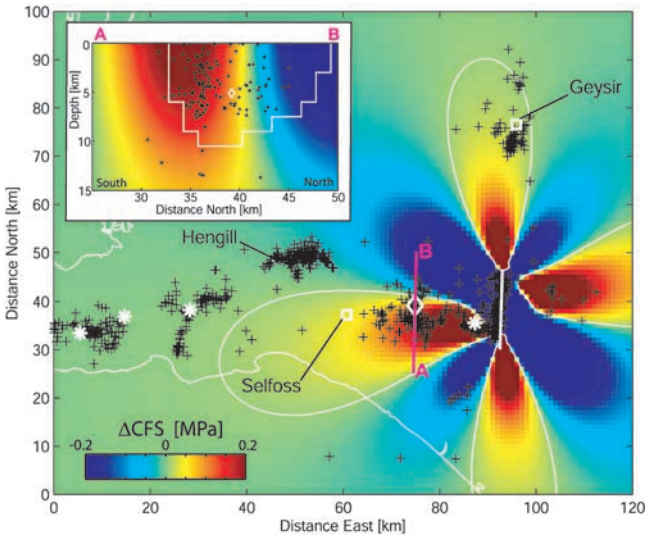

Figure 3. Static coseismic Coulomb failure stress changes (ΔCFS, in MPa) due to the June 17 fault slip (Figure 2), calculated at 5 km depth for vertical N-S faults with right-lateral strike slip motion. The contours surround areas where the *CFS* increased by more than 0.01 MPa (0.1 bar). The white diamond shows the location of the June 21 earthquake and white stars mark the largest aftershocks on June 17; note the three earthquakes triggered on Reykjanes Peninsula. Smaller aftershocks (location errors $\leq$2.5 km horizontally and $\leq$5 km vertically) with M $\geq$ 1.0, from June 17 to June 21, are shown with black crosses. The coastline and the location of the June 17 fault model are shown with white lines. The white squares mark the Geysir geothermal area and the town of Selfoss. The inset shows the ΔCFS in a N-S cross section along profile A-B. The extent of the June 21 fault is shown by the white box. Aftershocks from June 17 to June 21, located within 2.5 km east and west of the profile are shown with black crosses.

This area experienced a period of increased seismic activity from 1994–1998, which has been associated with uplift due to magma accumulation [*Sigmundsson et al.*, 1997; *Feigl et al.*, 2000]. The increase in seismicity at Hengill following the June 2000 earthquakes may have been dynamically triggered, as was observed at Long Valley Caldera following the 1992 Landers earthquake [*Hill et al.*, 1995]. Coseismic offsets observed on June 17 and 21, 2000, at continuous GPS stations located in the Hengill area can be explained by faulting in the SISZ and on Reykjanes Peninsula. No slow deformation signal suggesting resumed magmatic activity, could be detected in the Hengill area following the June 2000 earthquakes. Increased seismicity was also observed in the Geysir geothermal area (in a positive ΔCFS lobe in Figure 3, located due north of the June 17 rupture) following the June 17 mainshock.

[11] The calculated ΔCFS due to the June 17 mainshock, in a N-S cross section along the June 21 rupture, shows that the June 21 hypocenter is located where ΔCFS is positive (Figure 3 inset). Many earthquakes occurred in the June 21 fault zone during the time between the two mainshocks. It is arguable whether these earthquakes are June 17 aftershocks or June 21 foreshocks. Most of them are located in the area where ΔCFS is positive (Figure 3).

[12] The aftershock locations also correlate well with areas of increased Coulomb failure stress after the June 21 earthquake, particularly in the area between the two faults (Figure 4). The activity north of the two mainshocks appears to have extended westward in response to the increase in *CFS* following the June 21 earthquake. Less activity appears to have been triggered in the Hengill area (see Figure 4 inset) and on Reykjanes Peninsula following the June 21 earthquake, although it occurred closer to these areas than the June 17 event.

3. Discussion and Conclusions

[13] Calculations based on distributed slip models for the June 17 mainshock indicate that the earthquake caused an increase in the Coulomb failure stress in the June 21 hypocentral area of about 0.1 MPa, hence promoting failure on the June 21 fault. We obtain similar results (ΔCFS ranges from 0.09 to 0.13 MPa) using uniform slip models from *Árnadóttir et al.* [2001], *Pedersen et al.* [2001], and *Pedersen et al.* [2003], as well as for different values of μ ranging from 0.6 to 0.8, and B ranging from 0.2 to 1.0. Aftershock locations correlate well with areas of increased *CFS* following the two mainshocks. Increased seismicity in areas where ΔCFS was less than 0.01 MPa, such as on Reykjanes Peninsula and the Hengill volcanic area may have been dynamically triggered. Faulting may also have occurred on structures oriented more favorably to the stress changes in those areas than the N-S, right-lateral strike slip

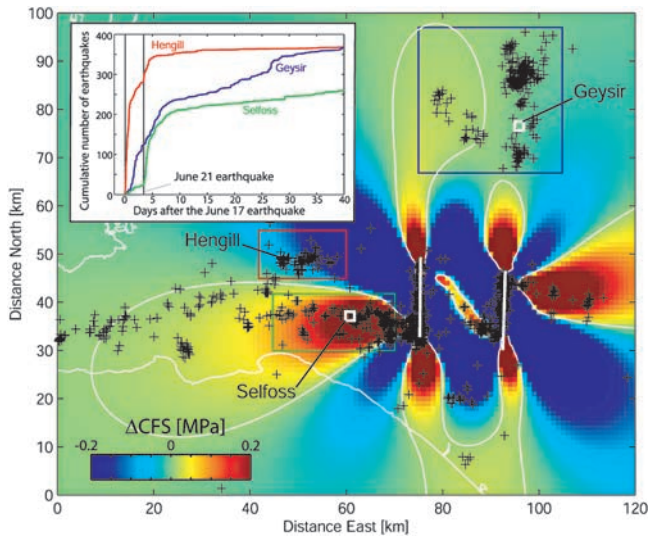

Figure 4. Static coseismic Coulomb failure stress changes (in MPa) due to both the June 17 and 21 earthquakes, calculated at 5 km depth for vertical N-S faults with right-lateral strike slip motion. The contours surround areas where the *CFS* increased by more than 0.01 MPa (0.1 bar). Aftershocks (M $\geq$ 1.0) from June 21 to December 31, 2000, are shown with crosses. The coastline and the location of the fault models are shown with white lines. The inset shows the cumulative number of earthquakes (M $\geq$ 1.0) in three areas, as a function of days after the June 17 mainshock. The locations of the areas are outlined with color boxes and labeled.

faults we asssume in our calculations. Focal mechanisms are not yet available to test that hypothesis.

[14] The June 17 and 21 earthquakes caused extensive surface ruptures [*Clifton and Einarsson*, 2000]. An E-W left-lateral structure in the surface rupture of the June 21 earthquake suggests complexities of the fault geometry that the geodetic data are unable to resolve [*Angelier and Bergerat*, 2002]. Relative relocation of aftershocks may provide information on details of the subsurface fault geometry. It is unlikely, however, that details of the fault geometry will change the basic conclusion of this study that the June 17 earthquake promoted failure on the June 21 fault.

[15] The importance of fluid flow in the SISZ in the June 2000 sequence was demonstrated by large coseismic pressure changes in water wells [*Björnsson et al.*, 2001], and rapid postseismic deformation due to poroelastic rebound after the two earthquakes [*Jónsson et al.*, 2002]. More sophisticated models that account for the effect of fluid flow may therefore be needed to explain the time delay of $3\frac{1}{2}$ days between the June 17 and 21 mainshocks.

[16] Figure 4 shows a large increase in *CFS* in an area extending west of the southern end of the June 21 rupture near the town of Selfoss, that correlates with a significant increase in seismicity following the June 21 mainshock. The last historical earthquakes in this area occurred in a sequence in 1896, with a M_S = 6.0 event on Sept. 5 (approximately 15 km west of the June 21 rupture), and an event of equal magnitude a day later approximately 10 km further west [*Stefánsson et al.*, 1993]. Our calculations indicate that positive stress changes due to the June 17 and 21 earthquakes make this area the most likely site of the next large SISZ earthquake.

[17] **Acknowledgments.** We thank two anonymous reviewers for their comments and suggestions. This work was supported in part by EU grant RETINA EVG1-CT-0044. Figure 1 was produced using the GMT public domain software.

References

Angelier, J., and F. Bergerat, Behaviour of a rupture of the 21 June 2000 earthquake in south Iceland as revealed in an asphalted car park, *J. Struct. Geol.*, *24*, 1925–1936, 2002.

Árnadóttir, T., S. Hreinsdóttir, G. Gudmundsson, P. Einarsson, M. Heinert, and C. Völksen, Crustal deformation measured by GPS in the South Iceland Seismic Zone due to two large earthquakes in June 2000, *Geophys. Res. Lett.*, *28*, 4031–4033, 2001.

Beeler, N. M., R. W. Simpson, S. H. Hickman, and D. A. Lockner, Pore fluid pressure, apparent friction, and Coulomb failure, *J. Geophys. Res.*, *105*, 25,533–25,542, 2000.

Bjarnason, I., P. Cowie, M. H. Anders, L. Seeber, and C. H. Scholz, The 1912 Iceland earthquake rupture: Growth and development of a nascent transform system, *Bull. Seismol. Soc. Am.*, *83*, 416–435, 1993.

Björnsson, G., Ó. G. Flovenz, K. Sæmundsson, and E. M. Einarsson, Pressure changes in Icelandic geothermal reservoirs associated with two large earthquakes in June 2000, paper presented at 26th workshop on Geothermal Reservoir Engineering, Stanford Univ., Stanford, Calif., 2001.

Clifton, A. E., and P. Einarsson, Styles of surface rupture accompanying the June 17 and 21, 2000 earthquakes in the South Iceland Seismic Zone, paper presented at Fall Meeting 2000, Geosci. Soc. of Iceland, 2000.

Cocco, M., and J. R. Rice, Pore pressure and poroelasticity effects in Coulomb stress analysis of earthquake interactions, *J. Geophys. Res.*, *107*(B2), 2030, doi:10.1029/2000JB000138, 2002.

Einarsson, P., and J. Eírksson, Earthquake fractures in the districts Land and Rangárvellir in the South Iceland Seismic Zone, *Jökull*, *32*, 113–120, 1982.

Einarsson, P., and K. Sæmundsson, Earthquake epicenters 1982–1985 and volcanic systems in Iceland, in *Í hlutarins edli*, edited by T. I. Sigfússon, Menningarsjódur, Reykjavík, 1987.

Einarsson, P., S. Björnsson, G. Foulger, R. Stefánsson, and T. Skaftadóttir, Seismicity pattern in the South Iceland Seismic Zone, in *Earthquake Prediction: An international review*, *Maurice Ewing Ser.*, vol. 4, edited by D. W. Simpson and P. G. Richards, pp. 141–151, AGU, Washington, D. C., 1981.

Feigl, K. L., J. Gasperi, F. Sigmundsson, and A. Rigo, Crustal deformation near Hengill volcano, Iceland 1993–1998: Coupling between magmatic activity and faulting inferred from elastic modeling of satellite radar interferograms, *J. Geophys. Res.*, *105*, 25,655–25,670, 2000.

Harris, R. A., Introduction to special section: Stress triggers, stress shadows, and implications for seismic hazard, *J. Geophys. Res.*, *103*, 24,347–24,358, 1998.

Hill, D. P., M. J. S. Johnston, and J. O. Langbein, Response of Long Valley caldera to the M_w = 7.3 Landers California, earthquake, *J. Geophys. Res.*, *100*, 12,985–13,005, 1995.

Jónsson, S., R. Pedersen, P. Segall, and G. Björnsson, Postseismic poroelastic deformation in South Iceland observed with radar interferometry: Implications for aftershock decay (abstract), *Eos Trans American Geophysical Union*, *83*(47), Fall Meet. Suppl., G62A-03, 2002.

Pagli, C., R. Pedersen, F. Sigmundsson, and K. Feigl, Triggered seismicity on June 17, 2000 on Reykjanes Peninsula, SW-Iceland captured by radar interferometry, *Geophys. Res. Lett.*, *30*, doi:10.1029/2002GL015310, in press, 2003.

Pedersen, R., F. Sigmundsson, K. Feigl, and T. Árnadóttir, Coseismic interferograms of two M_s = 6.6 earthquakes in the South Iceland Seismic Zone, June 2000, *Geophys. Res. Lett.*, *28*, 3341–3344, 2001.

Pedersen, R., S. Jónsson, T. Árnadóttir, F. Sigmundsson, and K. Feigl, Fault slip distribution of two M_s = 6.6 earthquakes in South Iceland from joint inversion of InSAR and GPS, *Earth Planet. Sci. Lett.*, in press, 2003.

Rice, J. R., and M. P. Cleary, Some basic stress diffusion solutions for fluid saturated elastic porous media with compressible constituents, *Rev. Geophys.*, *14*, 227–241, 1976.

Sigmundsson, F., P. Einarsson, S. T. Rögnvaldsson, G. R. Foulger, K. M. Hodgkinsson, and G. Thorbergsson, The 1994–1995 seismicity and deformation at the Hengill triple junction, Iceland: Triggering of earthquakes by minor magma injection in a zone of horizontal shear stress, *J. Geophys. Res.*, *102*, 15,151–15,161, 1997.

Spudich, P., L. K. Steck, M. Hellweg, J. B. Fletcher, and L. M. Baker, Transient stresses at Parkfield, California, produced by the M 7.4 Landers earthquake of June 28, 1992: Observations from the UPSAR dense seismograph array, *J. Geophys. Res.*, *100*, 675–690, 1995.

Stefánsson, R., R. Bödvarsson, R. Slunga, P. Einarsson, S. Jakobsdóttir, H. Bungum, S. Gregersen, J. Havskov, J. Hjelme, and H. Korhonen, Earthquake prediction research in the South Iceland Seismic Zone and the SIL project, *Bull. Seismol. Soc. Am.*, *83*, 696–716, 1993.

Toda, S., R. S. Stein, P. A. Reasenberg, J. H. Dietrich, and A. Yoshida, Stress transferred by the 1995 M_w = 6.9 Kobe, Japan, shock: Effect on aftershocks and future earthquake probabilities, *J. Geophys. Res.*, *103*, 24,543–24,565, 1998.

T. Árnadóttir and R. Pedersen, Nordic Volcanological Institute, Grensásvegur 50, IS-108 Reykjavík, Iceland. (thoral@lhi.is)

G. B. Gudmundsson, Icelandic Meteorological Office, Reykjavík, Iceland.

S. Jónsson, Department of Earth and Planetary Sciences, Harvard University, Cambridge, MA USA.